Bone 128 (2019) 115035

Contents lists available at ScienceDirect

Bone

journal homepage: www.elsevier.com/locate/bone

Full Length Article

The structure, composition and mechanical properties of the skeleton of the naked mole-rat (*Heterocephalus glaber*)

Shira Carmeli-Ligati[a], Anna Shipov[a], Maïtena Dumont[a], Susanne Holtze[b], Thomas Hildebrandt[b], Ron Shahar[a,*]

[a] Koret School of Veterinary Medicine, The Robert H. Smith Faculty of Agriculture, Food and Environmental Sciences, The Hebrew University of Jerusalem, PO Box 12, Rehovot 76100, Israel
[b] Department of Reproduction Management, Leibniz Institute for Zoo & Wildlife Research, Berlin, Germany

ARTICLE INFO

Keywords:
Bone
Remodeling
Mechanical properties
Naked mole-rats

ABSTRACT

The naked mole-rat (NMR) is a small rodent with a remarkable array of properties, such as unique physiology, extremely long life-span and unusual social life. However, very little is known regarding its skeleton. The aim of this study was to describe the structure, composition and mechanical properties in an ontogenetic series of naked mole-rat bones. Since common small rodents like mice and rats have an unusual structure of cortical bone, which includes a central region of non-lamellar (disordered) bone, mineralized cartilaginous islands and total lack of remodeling, this study could also determine if these are features of all small rodents.

Sixty-one NMRs were included in the study and were divided into the following four age groups: 0–0.5 years old (n = 17), 0.5–3 years old (n = 25), 3–10 years old (n = 13), and > 10 years (n = 6). Femora, vertebrae and mandibulae were examined using micro-CT, light microscopy, polarized light microscopy and scanning electron microscopy, thermogravimetric analysis was used to determine their dry ash content and their derived elastic modulus and hardness were determined using micro-indentation.

Our findings show that NMR bones are similar in composition and mechanical properties to those of other small rodents. However, in contrast to other small rodents, the cortical bone of NMRs is entirely circumferential-lamellar and lacks mineralized cartilage islands. Furthermore, despite their long life-span, their bones did not show evidence of remodeling at any of the age groups, thus proving that lack of cortical remodeling in small rodents is not caused by their short life-span, but characteristic of this order of mammals.

1. Introduction

The naked mole-rat (NMR), *Heterocephalus glaber*, has been studied intensively over the last three decades, due to its remarkable array of properties, such as unusual social life [1], very long life span [2–8], eco-physiological endurance and apparent resistance to neoplasia [9,10]. The NMR is a eusocial animal, naturally found in subterranean burrows in east Africa (Kenya, Ethiopia, and Somalia). It lives in large colonies (20–300 individuals) headed by one fertile queen [11], and with a clear division of class: reproducers and subordinate workers [1,12]. Workers maintain the colony by foraging for food [13,14], extending the burrow system [15], defending the colony and helping the queen care for her offspring. The queen and 1–3 reproductive males (named pashas) have longer life spans than workers and are the only sexually developed individuals in the colony. Nevertheless, females older than 6 months are capable of becoming reproductively active if the queen dies, and will fight to establish dominance [16,17]. The workers dig the elaborate burrow system in which the colony resides by using their hind limbs to brace themselves, and their teeth as chisels and digging tools. [4].

In order to be able to thrive in their subterranean niche, NMRs developed special physiological and morphological adaptations [3]. These include small eyes (with an expanded somatosensory cortex) and streamlined body shape which assists in movement within the burrows [3] and unusual respiratory physiology that enables them extreme tolerance of the hypoxic and hypercapnic atmosphere in their habitat [4,18]. Low body temperature, low metabolic rate, tolerance for vitamin D deficiency and efficient mineral metabolism in the absence of sunlight also enable NMRs to survive under harsh conditions [19,20].

The most remarkable observation associated with NMRs is their longevity [8]. The naked mole-rat is by far the longest-living rodent

* Corresponding author at: Laboratory of Bone Biomechanics, Koret School of Veterinary Medicine, The Robert H. Smith Faculty of Agriculture, Food and Environment, The Hebrew University of Jerusalem, Rehovot 76100, Israel.
E-mail address: Ron.shahar1@mail.huji.ac.il (R. Shahar).

https://doi.org/10.1016/j.bone.2019.115035
Received 26 June 2019; Received in revised form 8 August 2019; Accepted 9 August 2019
Available online 14 August 2019

known, with maximum life expectancy of > 30 years in captivity [6]. The life expectancy of the striped field mouse (in captivity) is only around 4 years [3].

Naked mole-rats experience minimal age-related changes in body composition, physiology, and molecular function, and retain good health and reproductive potential [17]. Such long life expectancy is particularly impressive when one considers their relatively small body size, compared to other mammals with such a long life span, like elephants (80 years) and some primates (30–60 years) [3,8]. For this reason, NMRs became a popular resource model to study age-related diseases [9].

Bone is a metabolically-active tissue, and one of its most remarkable features is its ability to remodel. During the process of remodeling small packets of tissue within the bulk are removed, and then replaced by new material, through the coupled activity of bone-resorbing cells (osteoclasts) and bone-building cells (osteoblasts). The most prevalent hypothesis for the need for remodeling cites local micro-damage accumulation [21,22]. While bone remodeling is present in almost all mammals, such that their entire skeleton is replaced every 4–10 years, the cortical bone of small rodents rarely remodels [23–25]. This is a surprising observation, considering the very fundamental nature of bone remodeling.

The cause for the lack of remodeling in the bones of small rodents is not clear, and two possible hypotheses have been put forward: (1) due to their small size, rodent bones do not require remodeling since the stresses they experience do not reach the limit of micro-damage generation. The weakness inherent to this explanation is that it implies that rodent bones are over-engineered, being unnecessarily bulky and therefore metabolically wasteful, a clear violation of the basic evolutionary principle of optimization, and therefore unlikely to be correct. (2) the short life span of small rodents does not allow micro-damage sufficient time to accumulate to a significant degree, and remodeling is therefore simply not required.

Relatively little has so far been published regarding the structure and mechanical properties of the skeleton of naked mole-rats [4,26]. Pinto and colleagues [26] studied the effect of sexual suppression on the structure of femora of NMR male and female breeders and non-breeders, and compared their morphometry, mineral density and whole bone stiffness. They did not find significant differences between subordinate and breeder males while femora of breeding females differed significantly from those of subordinate females. Edrey and colleagues [4] reviewed different aspects of NMR physiology, and make the comment that unlike mice their femora exhibit "…very efficient bone remodeling…". However, they base this conclusion on the observation of a few round objects in transverse sections of the femoral diaphysis (Fig. 1C, D in their paper), but these appear to us to be either primary osteons or blood vessels, and thus do not indicate remodeling.

The aims of this study were therefore to describe the structure, mechanical properties and mineral content of the skeleton of an ontogenetic series of naked mole-rat bones. In particular, we take advantage of the exceptionally long life-span of NMRs to examine whether the cortical bone material of this small rodent remodels, in contrast to other small rodents, with shorter life span, that do not.

2. Materials and methods

2.1. Animals

Naked mole-rat (*H. glaber*) colonies were kept at the Leibniz Institute for Zoo Biology and Wildlife Research, Berlin, Germany inside a climatized box (2x1x1 m) in artificial burrow systems, consisting of eight cylindrical acrylic glass containers (diameter: 240 mm height: 285 or 205 mm). The latter functioned as variable nest boxes, food chambers or toilet areas, and were interconnected with acrylic tubes having an inner diameter of 60 mm. Husbandry conditions were stable during the entire experimental period. Temperature and humidity were adjusted to 27.0 ± 2.0 °C and 85.0 + 5.0%, respectively. In general, the naked mole-rat (NMR) colonies were kept in darkness except for 2 to 4 h of daily husbandry activities. Fresh vegetable food was provided daily and ad libitum. In addition, commercial rat pellets (Vita special, Vitakraft GmbH, Bremen, Germany) were fed as an additional source of protein and trace elements. Animal housing and tissue collection at the Leibniz Institute for Zoo and Wildlife Research was compliant with national and state legislation (breeding allowance #ZH 156; ethics approval G 0221/12 "Exploring long health span", Landesamt für Gesundheit und Soziales, Berlin).

2.2. Specimens and sample preparation

At the end of an experiment unrelated to the skeletal system, sixty-one naked mole-rats were anaesthetized by 3% isoflurane inhalation anaesthesia (Isofluran CP, CP-Pharma, Burgdorf, Germany) and euthanized by surgical decapitation. Selected bones from these NMRs, which included femora, mandibles and lumbar vertebrae, were extracted and sent to the Bone Biomechanics Laboratory, Koret School of Veterinary Medicine, Israel. All bones were wrapped in a saline- soaked gauze pad and stored at $-20C^{\circ}$ until used for the various study techniques, at which time they were allowed to thaw slowly at room temperature.

The bones were, somewhat arbitrarily, divided into four age groups. The first group, 0–0.5 years old (n = 17, 11 females and 6 males), consisted of NMRs considered not to have reached sexual maturity, the second group consisted of 0.5–3 years old NMRs (n = 25, 15 females and 10 males), considered to be young adults, the third group consisted of 3–10 years old NMRs (n = 13, 9 females and 4 males), considered to be mature adults, and the fourth group consisted of old NMRs which were > 10 years old (n = 6, 3 females and 3 males). The cutoff age of 10 years was chosen based on the observation that only individuals older than 10 years had closed growth plates. In each age group representative samples of the three different bones, from both males and females, were examined.

2.3. Micro- CT scanning

Bones were scanned using a desktop Micro- CT scanner (Skyscan® 1174, micro-CT scanner, Skyscan, Belgium). Each bone was placed in a plastic tube and stabilized within agar to prevent movement during the scan. The X-ray source was set at 50 kVp and 800 μA. Scan parameters varied among the different types of bones and age of the individual (due to the differences in bone size and density). All specimens were scanned over 180 degrees with a rotation step of 0.4 degrees. A 0.25 mm aluminum filter was used to decrease beam hardening effects. The bones were scanned with an isotropic voxel size ranging between 7.5 and 13.7 μm^3 (determined by their size) and exposure times ranged between 2700 and 4200 s. We note that identical scanning parameters were used for all bones belonging to the same combination of bone type and age group. Scans were reconstructed and analyzed using commercial software (NRecon®, Bruker®, Kontich, Belgium and CT analyser®, Bruker®, Kontich, Belgium, respectively). Morphometric analysis and BMD (bone-mineral density) valuation were carried out on the cortical bone of femora and mandibulae using CTAn software (Skyscan® CT Analyser 1.13.5.1, Skyscan, Belgium).

Analysis of femora was performed in two regions: cortical analysis was carried out in the mid-diaphysis by measuring a region of interest (ROI) that was 2 mm long and centered around the mid- diaphysis, while trabecular analysis was carried out in the distal epiphysis, within a ROI starting at the edge of the growth plate for a distance of 0.5 mm. Jaw cortical analysis was carried out from the rostral edge of the mandible, where cortical bone begins to surround the lower incisor, 2 mm in the caudal direction. Lumbar trabecular analysis was carried out in the vertebral body by measuring a ROI extending 1 mm from the center. Three- dimensional representations of the various bones were

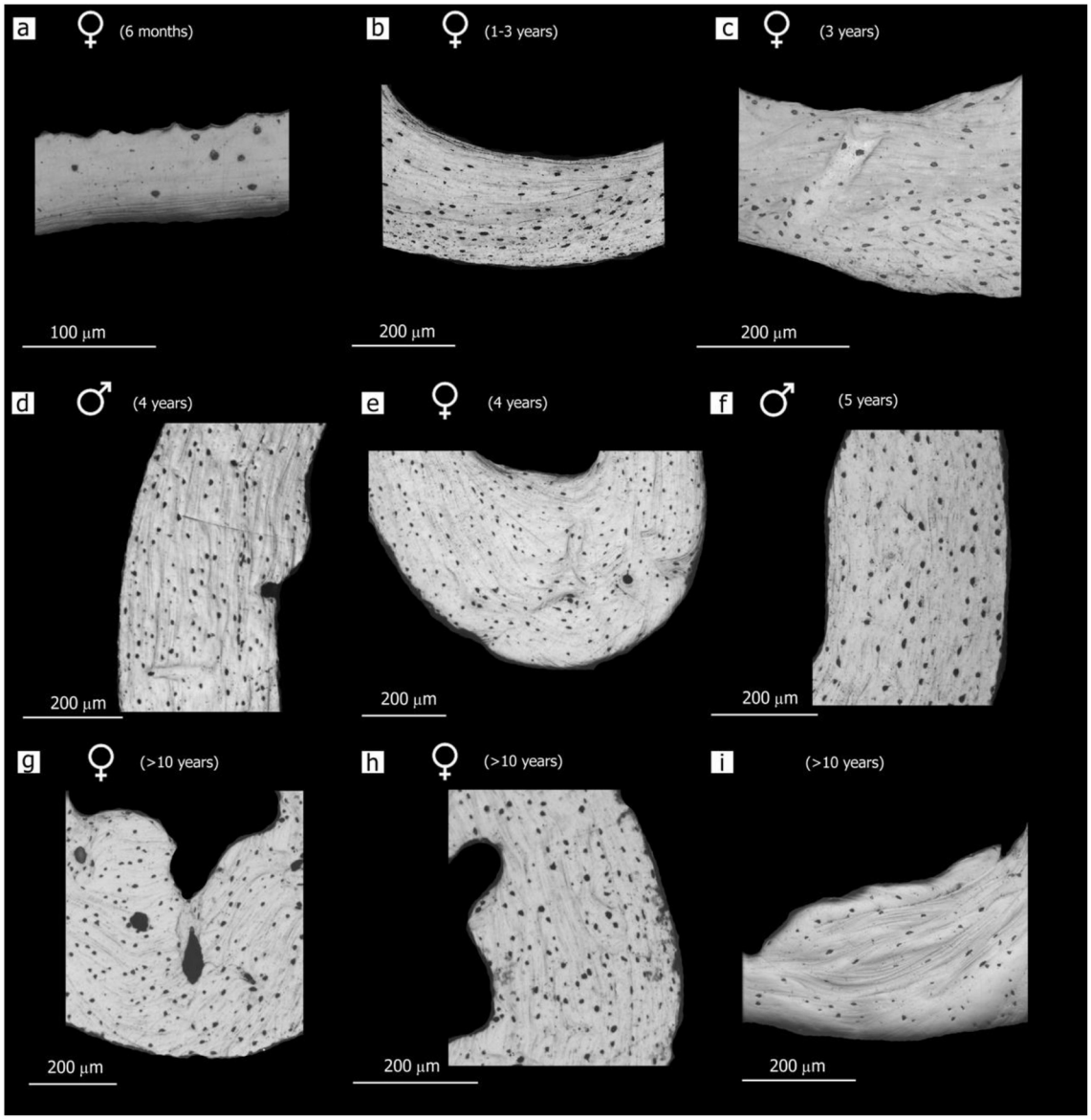

Fig. 1. a–i: Representative light microscopy images of regions in transverse cross-sections of femora from nine naked mole-rats of a variety of ages and sexes. Note high density of osteocytic lacunae coupled with paucity of blood supply, regardless of age and gender.

obtained utilizing a commercial visualization software (Amira, FEI, Hillsboro, Oregon, USA).

2.4. Light microscopy

Transverse (48) and coronal (33) sections were prepared from femora, and transverse sections were prepared from lumbar vertebrae (18) and mandibulae (18). Several bones from each age group were examined, excluding the youngest group, where bone size restricted the possibility of processing some samples.

The slices were cut using a slow-speed water-cooled diamond-blade saw (Isomet®, Buehler, Lake Bluff, Illinois, USA) to a thickness of approximately 1.5 mm. The slices were sequentially ground with 9 μm, 3 μm and 1 μm grit SiC films (Buehler, Lake Bluff, Illinois, USA), then polished with a nap cloth soaked with diamond suspension (3 μm, 1 μm and 0.25 μm, Struers, Westlake, Cleveland, USA). Sectioned surfaces were examined by a reflected-light microscope (Olympus® BX 51 microscope, Olympus, Tokyo, Japan) and images were obtained by a high-resolution dedicated camera (DP-71, Olympus, Tokyo, Japan).

2.5. Scanning electron microscopy (SEM)

Transverse and coronal slices from femora (n = 9) were embedded in epoxy resin and hardener (EpoThin™, Buehler, Illinois, USA), then prepared as described above and examined uncoated by scanning electron microscopes (JCM 6000, JEOL, Tokyo, Japan and the Phenom XL desktop SEM, Thermo Fisher Scientific, Eindhoven, The Netherlands), using the backscattered (BSE) detector with varying working distances, electron energy of 15 keV and high vacuum mode.

2.6. Polarized light microscopy

Coronal and transverse slices from two femora were prepared and polished to a thickness of ~150 μm, then examined using an LC-PolScope image processing system (CRi Inc., Woburn, MA, USA) mounted on a microscope (Nikon Eclipse 80i, Tokyo, Japan). Retardance images were taken by a cooled CCD camera at high optical resolution and retardance values were extracted using ABRIO software tools (CRi Inc., Woburn, MA, USA).

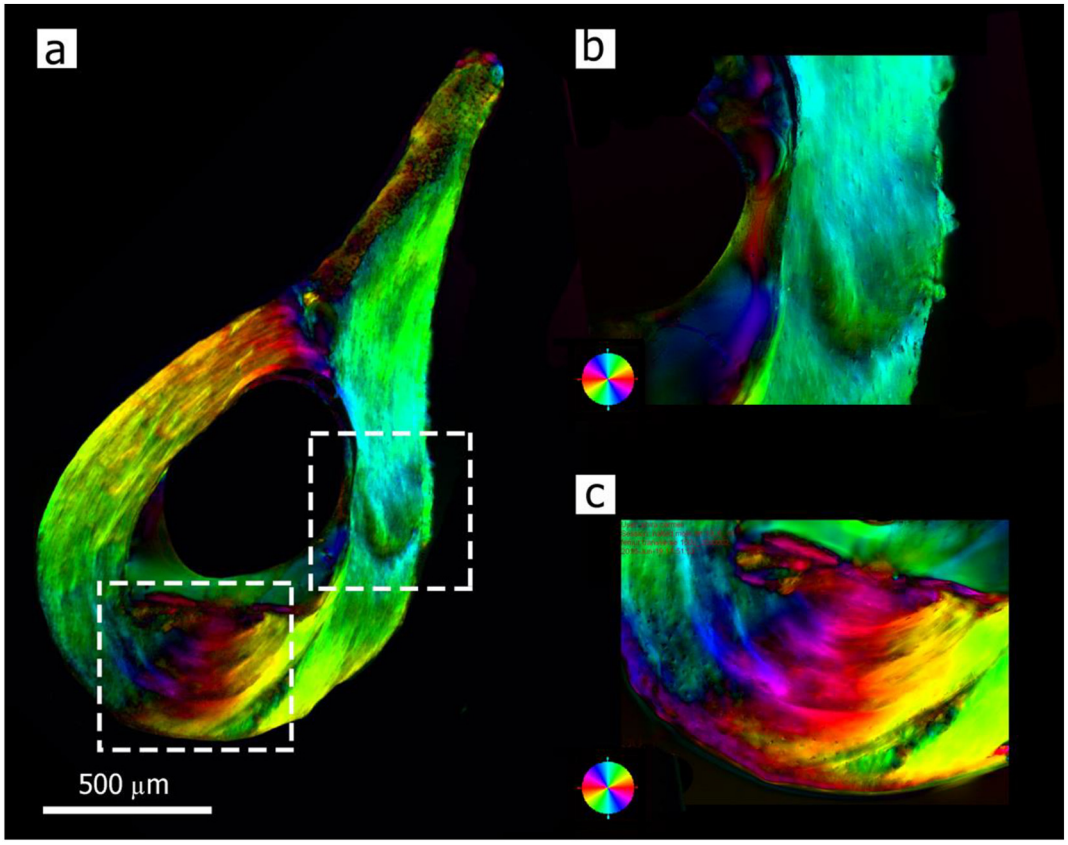

Fig. 2. Polarized light microscopy image of a typical transverse cross-section of a femur of a 3.5-year-old old female NMR. (a) In the entire section, the collagen fibers are seen to follow the circumferential orientation. (b, c) magnified insets of regions shown in (a). Circular color wheels code angular orientations, such that each color represents a directional vector and its 180^0 complement, as displayed in the color wheel.

Table 1
Blood vessel and lacunar density in the different age groups, presented as mean ± SD.

	0.5-3 years (n = 20)	3–10 years (n = 15)	> 10 years (n = 5)
Lacunar density (mm^{-2})	542.9 ± 111.2	553.2 ± 85.9	493.2 ± 132.1
Blood vessel density (mm^{-2})	2.21 ± 1.87	2.42 ± 1.98	1.63 ± 1.64

2.7. Micro-hardness

Transverse and coronal sections from 14 femora, belonging to the 0.5–3 years old group (n = 5), 3–10 years old group (n = 5) and > 10 years old group (n = 4) were tested using a micro-indenter equipped with a Vickers tip (FM 100, Future-Tech©, NY, USA). The sections were polished using the same protocol described above for microscopy. The polished samples were attached to the indenter stage and indentations were performed using 50 gf loading force and 10 s dwell time. Five to ten indentations were performed on each sample, making sure that the spacing between indentations exceeds three times the indentation width. Vickers hardness (HV) values ($kgf\,mm^{-2}$) were calculated using ARS 10 k software (Future-Tech©, NY, USA) via the formula:

$$HV = 1.8544 \times \left(\frac{F}{d^2}\right) \quad (1)$$

where F is the applied force and d is the average diagonal length of the indent in μm. The derived elastic modulus (E, GPa) was estimated from HV values via an empiric formula previously published for bone samples by Evans et al. [27] and later simplified by Daegling et al. [28]:

$$E = HV \times 0.36 + 0.58 \quad (2)$$

2.8. Ash content

Samples obtained from femora and mandibulae of six naked mole-rats, both females and males, from each age group were used for ash determination (the only exception were femora of the > 10 years old (5 samples) and mandibulae of the 0-0.5 year old and > 10 years old (3 samples)). Three small pieces (~1 mm in diameter) from each sample were grounded using mortar and pestle, then de-fatted with acetone for 6 h. A thermo-gravimetric analyser (Q500, TA Instruments, Delaware, USA) was used with the ramp method, at a heating rate of 10 °C per minute up to 600 °C. Analysis was carried out using the manufacturer's software (TA Universal Analysis 2000 TA Instruments, Delaware, USA).

2.9. Statistical analysis

Descriptive statistics were used and the results are expressed as mean and standard deviation. One-way ANOVA was used to compare continuous variables among all the age groups. When significant differences among all groups were found and the number of samples of each group category exceeded 6 samples, pairwise comparison between every pair of age groups was performed using the student's *t*-test with Bonferroni's correction. Statistical analysis was performed using a statistical software (IBM SPSS Statistics 25.0 for Windows, Chicago, IL, USA).

Fig. 3. Typical ontogenetic series of femoral transverse cross-sections of female NMRs. The transverse section of the 0–0.5 year old group shows a thin and irregular cortex, suggesting active modeling. The young mature cortex (0.5–3-year-old NMR) has smooth endosteal and periosteal borders, as does the section from the 3-year-old NMR, which however has a thicker cortex. The cortical section from the > 10 year old NMR, while thick, has irregular endosteal and periosteal borders, suggesting modeling. All sections, of all age groups, have numerous osteocytes, very few blood vessels and no secondary osteons.

Table 2
Morphometric properties of naked mole-rat cortical bone in the different age groups. Presented as mean ± SD.

	0–0.5 year (n = 11)	0.5–3 years (n = 23)	3–10 years (n = 12)	> 10 years (n = 4)
Medullary area (mm^2)	0.266 ± 0.239	0.394 ± 0.200	0.374 ± 0.168	0.458 ± 0.181
Cross-sectional bone area (mm^2) [a]	0.163 ± 0.099[b,c,d]	0.788 ± 0.288[c,d,e]	1.294 ± 0.214[b,e]	1.171 ± 0.174 [e]
Cross-sectional thickness (mm^2)[a]	0.062 ± 0.020[b,c,d]	0.230 ± 0.077[c,e]	0.317 ± 0.038[b,e]	0.263 ± 0.055[e]
Lacunar area (μm^2) [a]	56.9 ± 30.0	56.0 ± 26.0 [c,d]	53.2 ± 23.3[b,d]	50.4 ± 24.3[b,c]

[a] Significant difference among age groups.
[b] Significant difference from age group 2.
[c] Significant difference from age group 3.
[d] Significant difference from age group 4.
[e] Significant difference from group 1.

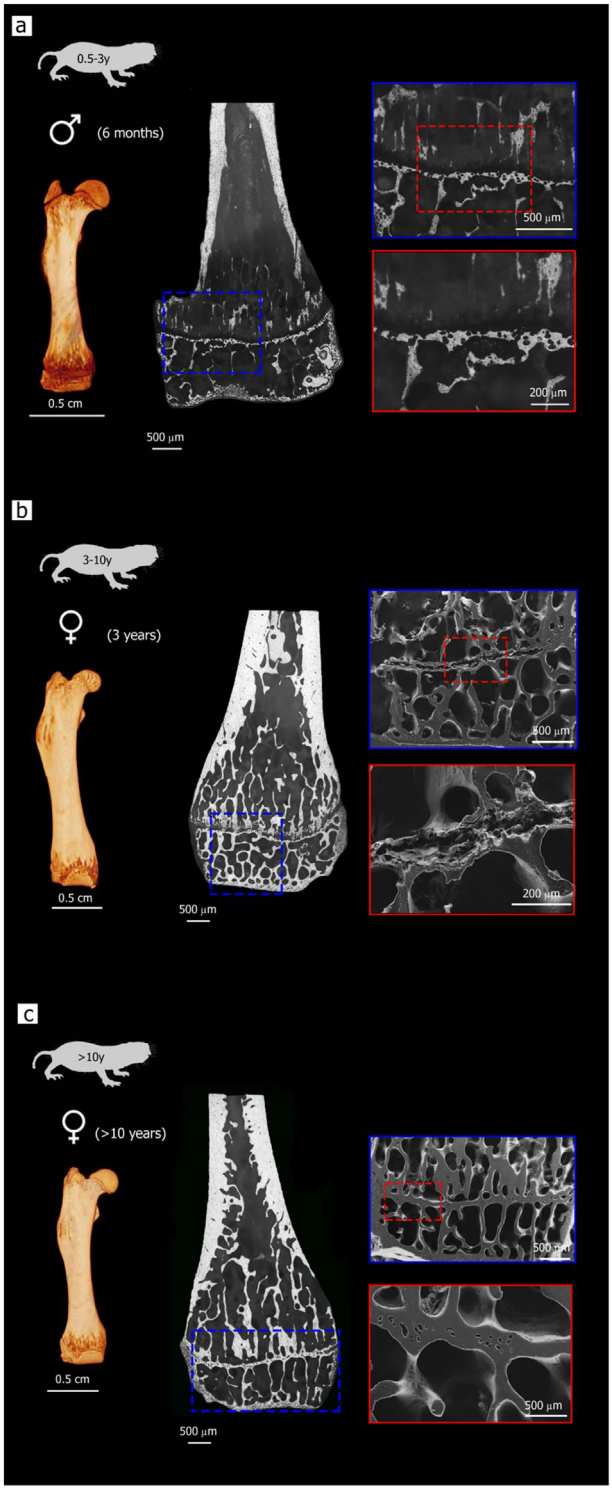

Fig. 4. Typical ontogenetic series of distal femoral coronal sections from male and female NMRs. (a, b) The sections belonging to NMRs < 10 years old have open growth plates, while the section of the > 10-year-old NMR shows a closed and mineralized growth plate.

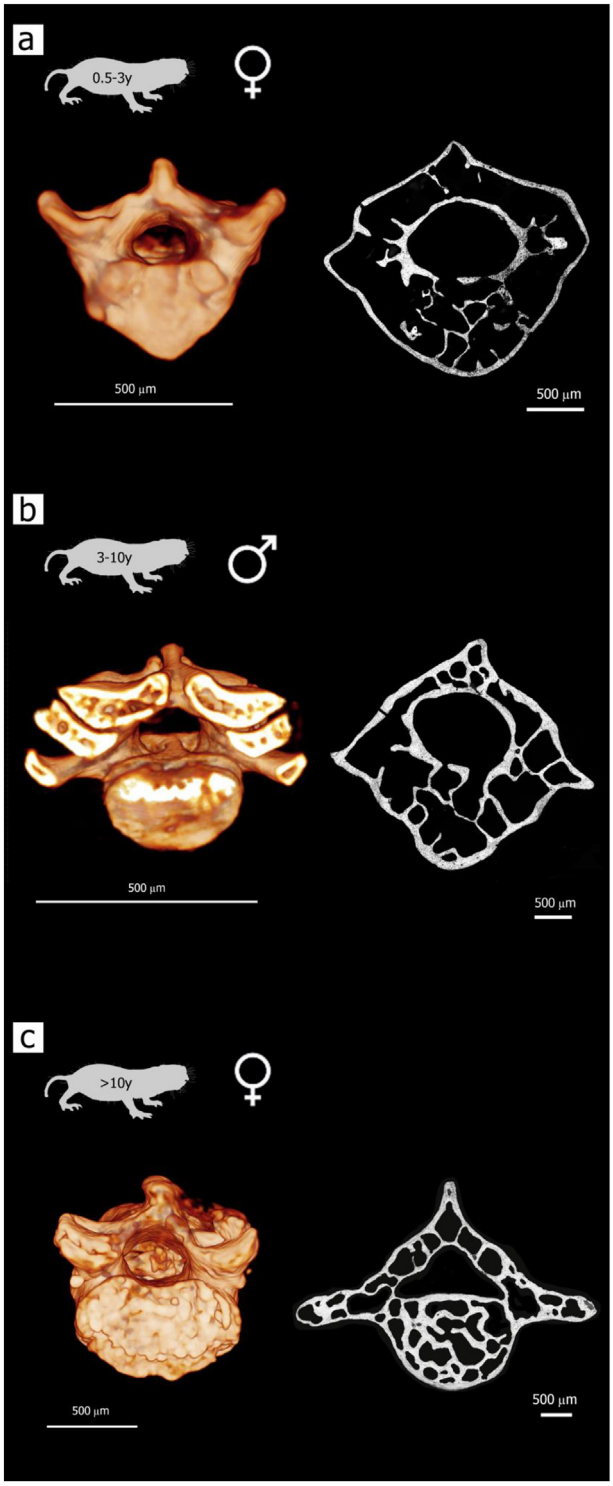

Fig. 5. Typical ontogenetic series of transverse cross-sections of lumbar vertebrae from an ontogenetic series of NMR. The intricacy of the cancellous bone increases from the very young (a) through the mature (b) to the old (c) NMR.

3. Results

3.1. Femoral cortical bone

Study of transverse sections of NMR femora by light microscopy shows that the cortical bone is composed entirely of circumferential lamellar bone, with sparse blood supply. This finding was consistent at all age groups examined, for both sexes. The bone matrix is densely populated with osteocytic lacunae that are aligned concentrically with the lamellae (see Fig. 1). Careful study of a large number of cross sections from cortical bone of femora from several NMRs belonging to each of the age groups failed to show even a single secondary osteon, thus confirming that the cortical bone of NMR does not undergo remodeling at any age (Fig. 1).

Transverse sections viewed by polarized microscopy show a

Table 3
Results of the morphometric analysis of cancellous bone from femora and vertebrae of NMRs in the different age groups.

Age		0–0.5 year Femora – n = 2, lumbar vertebra – n = 4	0.5–3 years Femora – n = 19, lumbar vertebra – n = 26	3–10 years Femora – n = 10, lumbar vertebra – n = 9	> 10 years Femora – n = 4, lumbar vertebra – n = 5
Femur	Trabecular separation (mm)	0.192 ± 0.038 n = 2	0.213 ± 0.023 n = 19	0.225 ± 0.036 n = 10	0.205 ± 0.024 n = 4
	Trabecular thickness (mm)[a]	0.060 ± 0.004[b,c] n = 2	0.079 ± 0.013 n = 19	0.088 ± 0.008[d] n = 10	0.092 ± 0.007[d] n = 4
	% bone volume	20.7 ± 3.2 n = 2	26.7 ± 6.6 n = 19	29.6 ± 5.5 n = 10	34.0 ± 1.8 n = 4
Lumbar	Trabecular thickness (mm)[a]	0.056 ± 0.008 n = 4	0.085 ± 0.026 n = 26	0.093 ± 0.009 n = 9	0.103 ± 0.0151 n = 5
	Trabecular separation (mm)	0.247 ± 0.032[b,c] n = 4	0.268 ± 0.059 n = 26	0.265 ± 0.045[d] n = 9	0.254 ± 0.0279[d] n = 5
	% bone volume[a]	12.9 ± 4.3[b,c] n = 4	23.5 ± 10.3 n = 26	30.0 ± 3.2[d] n = 9	33.6 ± 5.50[d] n = 5

[a] Significant difference among age groups.
[b] Significant difference from age group 3–10 yr.
[c] Significant difference from age group > 10 yr.
[d] Significant difference from group 0–0.5 yr.

circumferential pattern of collagen fiber orientation within the bone lamellae (see Fig. 2). Collagen fiber orientation changes progressively along the circumference, such that it is co-aligned with the lamellae and the external bone contour.

Results of quantitative analysis of osteocytic lacunar density and vascular channel density of all age groups are presented in Table 1. Area lacunar density of all samples from all age groups was found to be $532.8 \pm 114\,mm^{-2}$, with no statistically significant difference among age groups ($P = 0.54$). Blood vessel density of all samples from all age groups was found to be quite sparse ($2.22\,mm^{-2} \pm 1.90\,mm^{-2}$), with no statistically significant difference among the age groups ($P = 0.74$).

An ontogenetic series of transverse cross-sections of femora of female NMRs belonging to different age groups is presented in Fig. 3, and a quantitative evaluation of changes in the morphological parameters of cortical bone during ontogeny are presented in Table 2. These results show a significant difference between the age groups in mean cross-sectional area and thickness ($P < 0.001$), with a consistent increase from very young NMRs (0–0.5-year-old) to adults (3–10 years old) NMRs (Table 2). However, once the age exceeds 10 years the cross-sectional area decreases, mostly due to endocortical resorption. Lacunar area gradually decreases from young adulthood to senescence (Table 2).

An ontogenetic series of coronal sections of distal femora of male and female NMRs belonging to different age groups is presented in Fig. 4. The coronal sections allow examination of the distal femoral epiphyseal growth plate, and how it changes with age. As can be seen in Fig. 4, at the age of 3 years the epiphyseal growth plate is still open, though at this age minimal growth occurs. This pattern was observed even in older age (up to 10 years in our samples), while only in bones obtained from NMRs older than 10 years old, the epiphyseal growth plate was found to be closed.

3.2. Cancellous bone

Cancellous bone was analyzed in femora and lumbar vertebrae. Fig. 5 illustrates a typical ontogenetic series of light microscopy images of lumbar vertebrae. The images display an intricate trabecular network that develops with age. In mature animals (3–10 years old) the trabecular arrangement is more intricate and trabeculae are thicker than those in the younger group (0.5–3 years old), while in sections from vertebrae of old NMRs (> 10 years old), the trabecular network becomes quite irregular. The cortical bone of the vertebral body is composed of lamellar bone.

Quantitative analysis shows that trabecular thickness changes significantly among the different age groups ($P = 0.015$) with the youngest group having significantly thinner trabeculae compared to mature adults ($P = 0.042$) and the > 10 years group ($P = 0.015$). In the femur, the differences between the groups did not reach statistical significance. There was no change in trabecular separation (mean distance between trabeculae, assessed in 3-D) among the age groups both in the femur and the lumbar cortical bone (Table 3).

3.3. Mandibular bone

Fig. 6 displays an ontogenetic series of transverse sections of mandibulae. Mandibular samples did not exhibit any secondary osteons in the cortical bone; this finding indicates complete absence of bone remodeling. The mandibular bone is lamellar, and seems less organized than the pattern noted in femora. 3D representation of mandibulae of NMRs shows the overall appearance of the mandible, molar teeth and incisors. The incisors consist of a dentinal core and a thick anterior enamel layer. Transverse sections at the rostral part of the mandible of the youngest (0–0.5 years) and oldest age groups (> 10 years) reveal lamellar bone, as well as a dense network of blood vessels. The incisors appear to extend very far caudally, with the root extending well beyond the molars.

3.4. Bone mineral density

Bone mineral density values of the femoral and mandibular cortical bone are presented in Fig. 7. The analysis revealed a significant difference in BMD among all age groups ($P < 0.001$). Specifically, the youngest group had the lowest BMD compared to all other groups, ($P < 0.001$), while the young adult group (0.5 years to 3 years old) had lower BMD compared to the mature group (3–10 years old, $P = 0.036$), but not the old NMRs (> 10 years old). Compared separately, the difference between the BMD of mature and old NMRs did not reach statistical significance. The BMD values of the mandibular cortical bone also exhibit a similar trend. The impact of sex on these data would be of interest but the small sample numbers, when divided into sex, bone type and age group did not allow a valid statistical analysis.

3.5. Dry bone ash content

No significant differences were found in the ash content of cortical bone of the femora and mandibulae among the different age groups ($P = 0.237$ and $P = 0.624$, respectively, Fig. 8). The large variation observed in the ash % in the femora of the 0–0.5 years old group probably results from the rapid changes in mineralization of the developing skeleton at this age group.

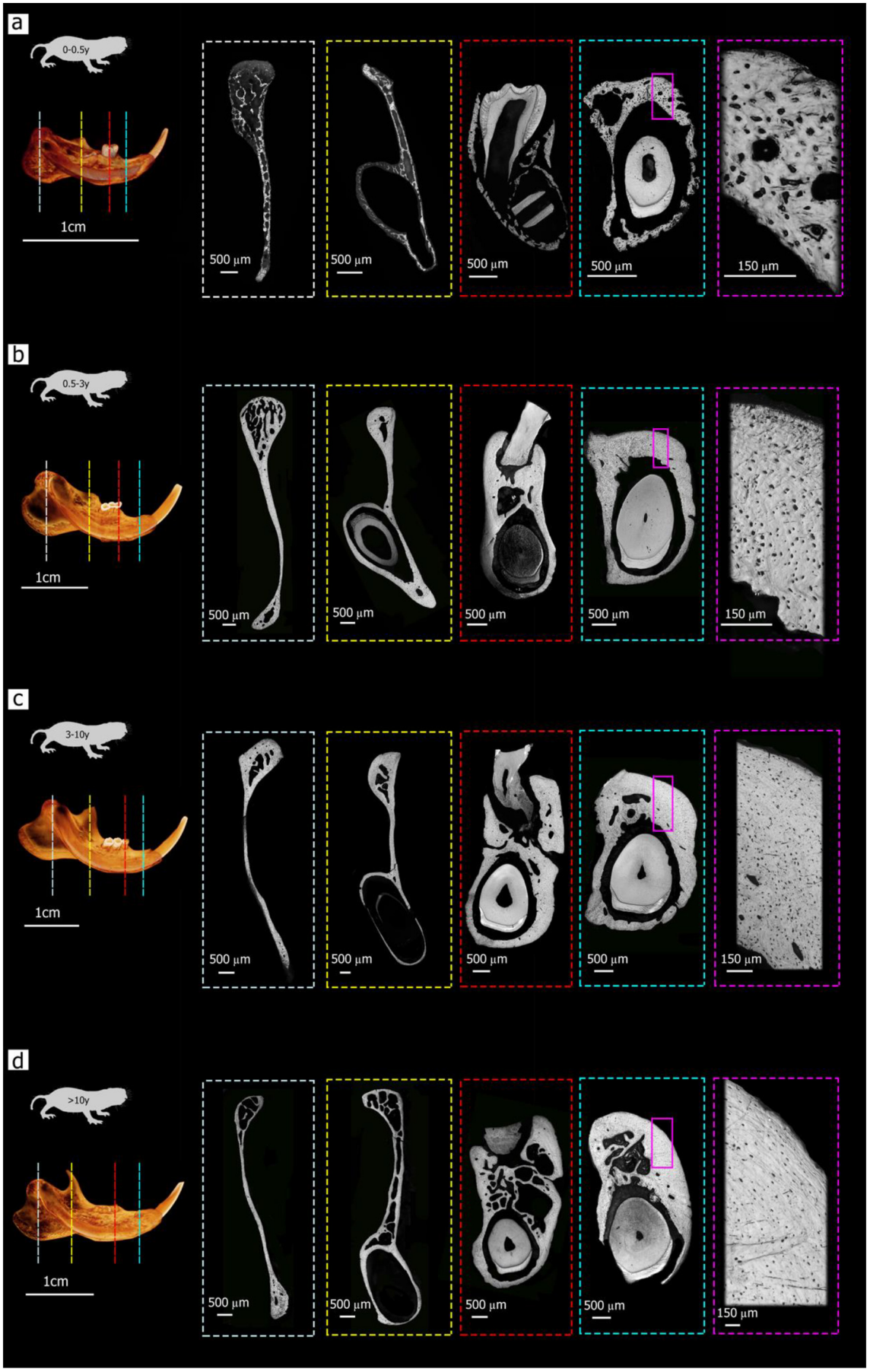

(caption on next page)

Fig. 6. Typical ontogenetic series of transverse cross-sections of mandibulae, at different locations along the caudo-cranial axis (a–d). The sections show the cross section of the incisor with an anterior enamel cap which is highly mineralized, and a less mineralized dentinal bulk. The incisors are surrounded by the mandibular bone. The last column shows insets from the mandibular cortical bone, which do not show evidence of remodeling, as noted by the complete absence of secondary osteons. One of the slices (mid-position, red rectangle) includes a section of one of the molar teeth. (For interpretation of the references to color in this figure legend, the reader is referred to the web version of this article.)

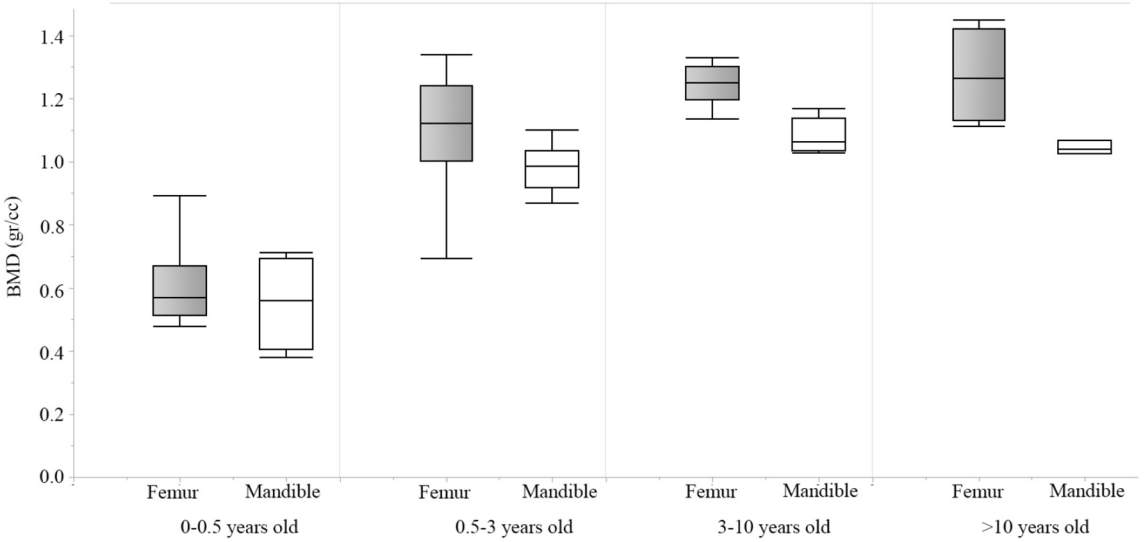

Fig. 7. Box plot representations of the femoral and mandibular BMD in the different age groups. Significant differences were found among the different groups, as described in the text. Most notably, The very young group (0–0.5 years old) had lower BMD values compared to all other groups as expected. The trends noted were similar in the femora and mandibulae.

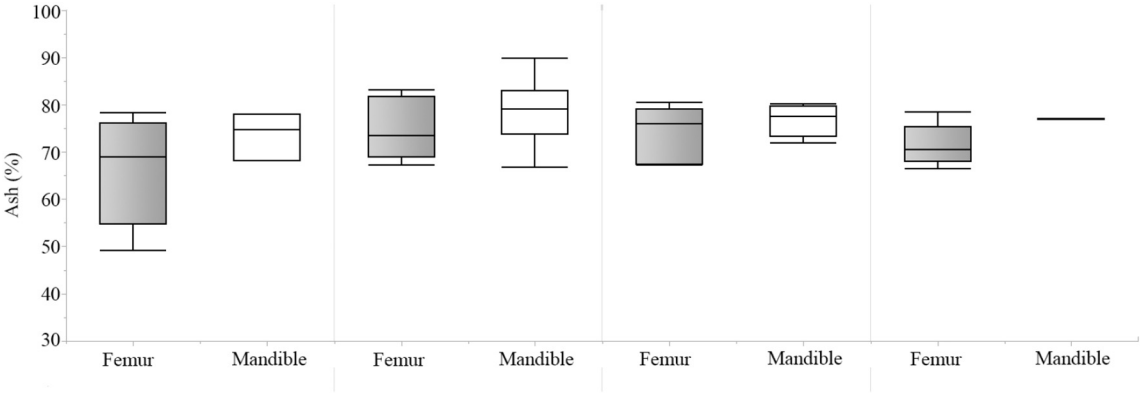

Fig. 8. Box plot representations of the femoral and mandibular ash % in the different age groups. There was no significant difference between the different age groups in both femora and mandibulae.

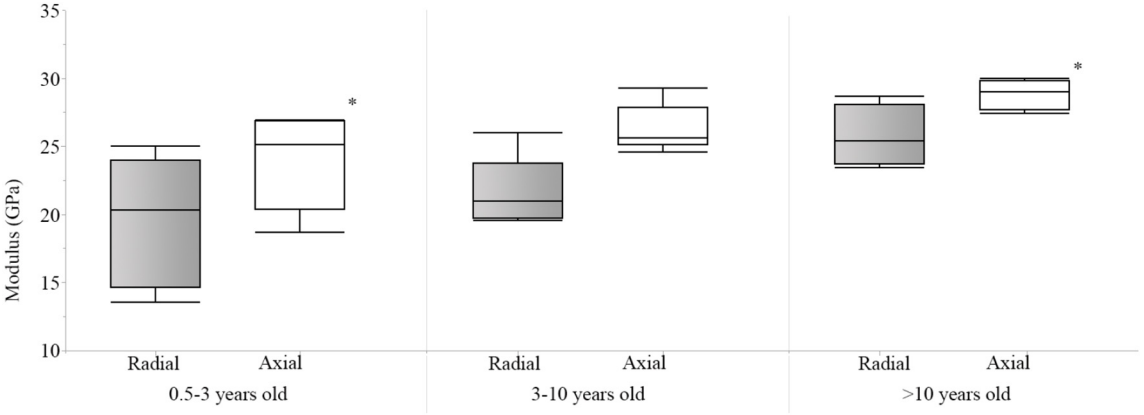

Fig. 9. Box plot representations of the derived elastic moduli of femoral cortical bone in two orthogonal orientations, in the different age groups. Derived moduli in the axial orientation tend to be higher than those in the radial orientation, but this tendency was not statistically significant.

Table 4
Comparison of mineral density, dry bone ash % and indentation-derived elastic moduli between NMRs and values published in the literature for rat and mouse cortical bone [23,25,29–37].

	BMD	Ash	Derived elastic modulus
Mouse	1.35 g/cc [29]	64.7% [32]	~25 GPa [31]
	1.24 g/cc [30]	65.9% [33]	~22 GPa [35]
	1.10 g/cc [31]		
Rat	1.25 g/cc [36]	62.2% [34]	27.8 GPa [25]
	1.33 g/cc [37]		24.5 GPa [23]
	1.36 g/cc [25]		
NMR	~1.20 g/cc	~70%	26.18 GPa

3.6. Mechanical properties of the femoral cortical bone

Fig. 9 presents results of micro-hardness testing conducted on femoral cortical bone samples and their conversion to derived elastic moduli. The hardness and derived elastic modulus in the two indentation orientations (axial and radial) can be seen to increase with age, however the difference between the age groups did not reach statistical significance for indentations in the radial orientation ($P = 0.064$). For indentations in the axial orientation, the only statistically-significant difference was found between the derived elastic modulus of animals belonging to the old group compared to the young adult group ($P = 0.036$, Fig. 8). When the derived elastic modulus is compared between the axial and radial orientations, the derived axial modulus is consistently higher than the derived radial modulus, as expected (26.18 ± 3.04 vs. 22.0 ± 4.13, respectively, $P < 0.001$).

Table 4 compares the values we report here for bone composition and mechanical properties with similarly reported values for mice and rat cortical bone.

4. Discussion

Here we describe the structure, composition and mechanical properties of bones in the skeleton of an ontogenetic series of the naked mole-rat *Heterocephalus glaber*. Our findings show that NMR bones are similar in composition and mechanical properties to those of other small rodents, but their structure is different. Despite the fact that NMRs have a very long life span, their bones do not undergo remodeling, as is the case in mice and rats whose life span is considerably shorter. We thus conclude that lack of remodeling in small rodents is characteristic of this order of mammals.

The primary architectural motif of cortical bone in the skeletal elements of the NMR skeleton studied here is circumferential lamellar, regardless of their age (Fig. 3) and sex (Supplementary Fig. 1). This finding contrasts with the structure of cortical bone in long bones of rats and mice, which is composed of two distinctly different architectural motifs, consisting of disordered bone, usually found in the central part of the cortex, flanked by endosteal and periosteal circumferential lamellar bone. [23,25].

Another feature, found consistently in the disordered regions in cortical bone of rats and mice are calcified cartilaginous islands, hypothesized to results from lack of resorption of the mineralized growth plate during endochondral bone formation in small rodents. [23,25]. However, this feature is entirely absent in the cortical bone of NMRs (see Fig. 10).

The cortical bone of naked mole-rats of all ages was found to have relatively sparse blood supply, with the area density of the blood vessels very low compared to other mammals, and specifically compared to small rodents (based on subjective comparison of transverse femoral sections of NMRs and similar sections we obtained in the past from femora of horses, dogs, cats and rats – data not shown). Such limited blood supply would suggest a low metabolic rate. Low metabolic rate would be expected to be associated with small cellular density, yet the density of osteocytic lacunae is quite high ($532.8 \pm 114\,mm^{-2}$), higher than reported values of $250–400\,mm^{-2}$ in dogs [38] and somewhat lower than the reported values in rats ($800\text{-}1760\,mm^{-2}$) [38–40]. The most widely accepted role proposed for osteocytes suggests that their wide distribution and large numbers within the bone matrix, combined with their connectivity with neighboring osteocytes through the lacuno-canalicular system make them perfectly suited to be sensors of the mechanical environment within the bone and enable them to efficiently regulate bone remodeling. Since despite the high density of osteocytes in NMR bones no evidence of remodeling was found, we assume that other proposed roles, such as mineral homeostasis [41], nutrient support and signal transmission [42,43] may be more important in this species.

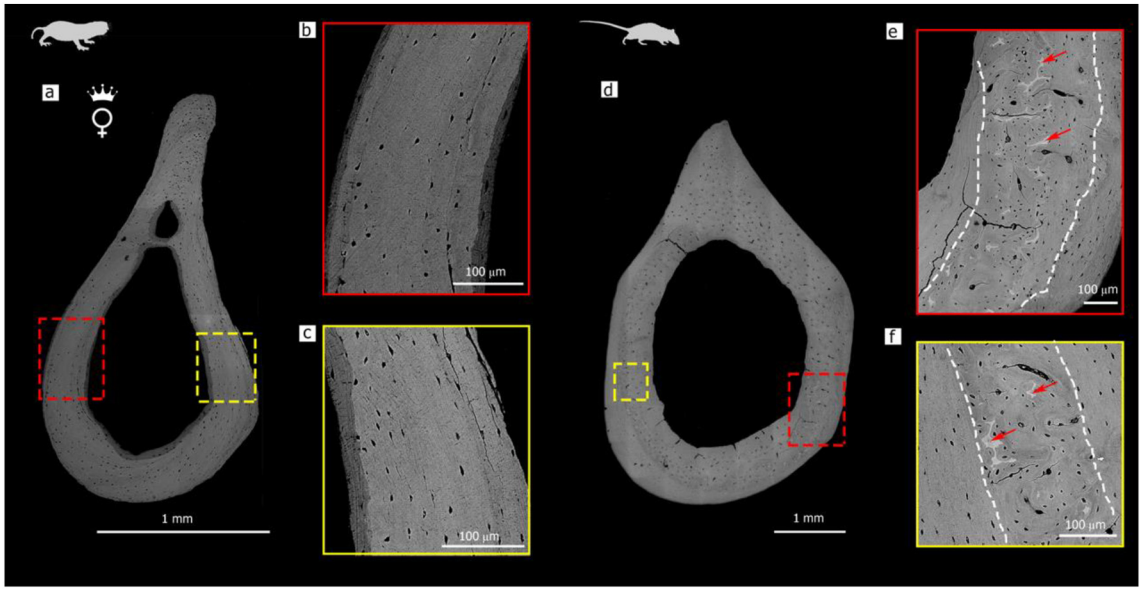

Fig. 10. Scanning electron microscopy images (back scattered detector) showing a comparison of mid diaphyseal transverse section of femora of (a) NMR and (b) rat. Note simple circumferential lamellar architecture of NMR bone, while in the rats ordered architecture is seen in the endosteal and periosteal regions, while the central region (demarcated with dotted lines) is disordered and contains hyper-mineralized islands (red arrows). (For interpretation of the references to color in this figure legend, the reader is referred to the web version of this article.)

The lack of remodeling in the bones of small rodents is intriguing [24,25,44]. Bone remodeling is found in almost all mammals, and has been suggested to allow replacement of old and damaged bone material with new, pristine bone. One of the explanations offered for this lack of remodeling was that due to their small size, rodent bones do not require remodeling since the stresses they experience do not reach the limit of micro-damage generation. However, such an explanation leads to the conclusion that rodent bones are over-designed, that is, they could function well with thinner cortices, and therefore are not metabolically optimized. This hypothesis contradicts several studies which have shown that terrestrial mammal's limb bones scale to body mass such that a uniform safety factor of a yield stress that is at least 3 times the peak physiological stress is maintained regardless of animal's size [45–49]. Therefore, the bones of rodents are expected to be subjected to similar strains as bones of larger animals and would thus also require remodeling to avoid damage accumulation and risk of failure.

Another hypothesis to explain lack of remodeling in rodent bones arose during discussions with John Currey, who suggested that it could be due to their short life span, which does not allow significant damage to accumulate. However, this explanation is refuted by the results of this study, since NMRs have a relatively long life expectancy, and their bones could be expected to accumulate damage and therefore would need to remodel to avoid failure. Yet we did not find any evidence of remodeling in their bones. Future studies are planned to evaluate the amounts of micro-damage accumulation in the bones of NMRs and compare those to microdamage accumulation in bones of other mammals where remodeling does occur.

Mineralization of the skeleton of NMRs proceeds in a pattern similar to that of other mammals. The long bones of immature NMRs (< 6 months old) are poorly mineralized, allowing them elasticity and toughness, with average bone mineral density (BMD) of 0.56 g/cc. As they mature their BMD increases, reaching a mean of 1.09 g/cc in young adults and finally stabilizing in adults at approximately 1.25 g/cc. These levels are similar to those reported in mice and rats (see Table 4).

Ash content is another parameter which is important in terms of bone composition. This parameter describes the weight percent of the mineral component in bone, and thus has implications with regard to the organic/inorganic ratio. Dry bone ash % was found to be remarkably consistent in all bones examined (mandibulae, and femora), with values ranging around 70%. This ash content is somewhat higher than values reported in rats and mice. This difference may be due to differences in measurement methodologies.

Although we did not find evidence for remodeling (replacement of small packages of bone material within the bone bulk), our results indicate an active and ongoing process of modeling (adaptation of the external and internal bone surfaces to changing load conditions) of NMR long bones. In adolescent NMRs cortical thickness and area are relatively small, adapted to their lower weight and limited activity at this age range. As they mature, cortical thickness and cross-sectional area increase. Since the medullary area tends also to increase, these results suggest that bone material is added periostealy, increasing whole bone bending strength, as the cross-sectional moment of inertia is proportional to the 4th power of the distance of the neutral axis from the geometric center. A similar trend of modeling was also observed in the trabecular bone of lumbar vertebra, where mean trabecular thickness and percent bone volume were smaller in adolescents compared with the same parameters in adults.

The mechanical properties of the bone material of mature NMRs are similar to those of other mammals. The hardness values at the 3 age groups of adult NMRs examined here (0.5 years − 3 years, 3 years-10 years and > 10 years) tended to increase with age, however, this difference did not reach statistical significance (P = 0.064), with mean values of derived modulus in the range of 20–25 GPa.

Growth plate closure in the long bones of mammals usually occurs around the time they reach sexual maturity. In this study, we found that the distal femoral growth plate of NMRs remains open at least for the first 10 years of life. In fact, we only observed closed growth plates in individuals older than 10 years (Fig. 4 and Supplementary Figs. 2 and 3). Growth plate closure is a complex phenomenon, primarily regulated by sex hormone levels. It is possible that growth plate closure in naked mole-rats is delayed due to suppression by the queen. Subordinate female NMRs have immature gonads and low levels of circulating sex hormones as long as they are under the reproductive suppression [50,51]. Interestingly, when a female colony member is separated from the colony, reproductive suppression is removed, and it experiences substantial longitudinal growth; however, this growth is attributed mostly to elongation of the vertebrae, not the long bones [52].

In summary, this study presents the structural and mechanical properties of the NMR, demonstrating similarities to other rodents in terms of composition, mechanical properties, growth patterns and basic bone structure. However, this bone does not contain un-remodeled calcified cartilaginous islands. Furthermore, the bone of this long-living rodent shows no evidence of remodeling, suggesting that the remodeling process is not a characteristic feature of bones of this order of mammals.

Supplementary data to this article can be found online at https://doi.org/10.1016/j.bone.2019.115035.

Acknowledgements

We are grateful to Professor Filipe Natalio, Dr. Emeline Raguin and Dr. Lior Ofer for their assistance with scanning electron microscopy, and Professor Rivka Elbaum and Mrs. Efrat Ziv for assistance with polarized light microscopy; RS was supported by Israel Science Foundation (ISF) grant # 29/12.

Author contribution

TH, SH established the NMR colony, obtained the samples. SCL and RS designed the study; SCL and RS acquired microscopy images, microCT scans and performed micro-indentation testing; SCL, AS, MD and RS quantified data; SCL and MD created figures; SCL, MD, TH, SH and RS prepared the manuscript; all authors read and approved the manuscript.

Declaration of competing interest

The authors declare no conflict of interest.

References

[1] J. Jarvis, Eusociality in a mammal - cooperative breeding in naked mole-rat colonies, Science 212 (1981) 571–573, https://doi.org/10.1126/science.7209555.
[2] M. Bens, K. Szafranski, S. Holtze, A. Sahm, M. Groth, H.A. Kestler, et al., Naked mole-rat transcriptome signatures of socially suppressed sexual maturation and links of reproduction to aging, BMC Biol. 16 (2018) 1–13, https://doi.org/10.1186/s12915-018-0546-z.
[3] R. Buffenstein, The naked mole-rat: a new long-living model for human aging research, J. Gerontol. Biol. Sci. 60A (2005) 1369–1377, https://doi.org/10.1093/gerona/60.11.1369.
[4] Y.H. Edrey, M. Hanes, M. Pinto, J. Mele, R. Buffenstein, Successful aging and sustained goodhealth in the naked mole rat: a long-lived mammalian model for biogerontology and biomedical research, ILAR J. 52 (2011) 41–53.
[5] I. Heinze, M. Bens, E. Calzia, S. Holtze, O. Dakhovnik, A. Sahm, et al., Species comparison of liver proteomes reveals links to naked mole-rat longevity and human aging, BMC Biol. 16 (2018) 1–18, https://doi.org/10.1186/s12915-018-0547-y.
[6] J.G. Ruby, M. Smith, R.B. elife, Naked mole-rat mortality rates defy Gompertzian laws by not increasing with age, eLIFE (2018), https://doi.org/10.7554/eLife.31157.001 n.d..
[7] A. Sahm, M. Bens, K. Szafranski, S. Holtze, M. Groth, M. Görlach, et al., Long-lived rodents reveal signatures of positive selection in genes associated with lifespan, PLoS Genet. 14 (2018), https://doi.org/10.1371/journal.pgen.1007272 (e1007272-23).
[8] V.P. Skulachev, S. Holtze, M.Y. Vyssokikh, L.E. Bakeeva, M.V. Skulachev, A.V. Markov, et al., Neoteny, prolongation of youth: from naked mole rats to “naked apes” (humans), Physiol. Rev. 97 (2017) 699–720, https://doi.org/10.1152/

physrev.00040.2015.
[9] A. Seluanov, C. Hine, J. Azpurua, M. Feigenson, M. Bozzella, Z. Mao, et al., Hypersensitivity to contact inhibition provides a clue to cancer resistance of naked mole-rat, Proc. Natl. Acad. Sci. 106 (2009) 19352–19357, https://doi.org/10.1073/pnas.0905252106.
[10] X. Tian, J. Azpurua, C. Hine, A. Vaidya, M. Myakishev-Rempel, J. Ablaeva, et al., High-molecular-mass hyaluronan mediates the cancer resistance of the naked mole rat, Nature 499 (2013) 346–349, https://doi.org/10.1038/nature12234.
[11] K. Roellig, B. Drews, F. Goeritz, T.B. Hildebrandt, The long gestation of the small naked mole-rat (Heterocephalus glaber RÜPPELL, 1842) studied with ultrasound biomicroscopy and 3D-ultrasonography, PLoS One 6 (2011), https://doi.org/10.1371/journal.pone.0017744 (e17744–10).
[12] E.C. Henry, C.M. Dengler-Crish, K.C. Catania, Growing out of a caste - reproduction and the making of the queen mole-rat, J. Exp. Biol. 210 (2007) 261–268, https://doi.org/10.1242/jeb.02631.
[13] T. Debebe, E. Biagi, M. Soverini, S. Holtze, T.B. Hildebrandt, C. Birkemeyer, et al., Unraveling the gut microbiome of the long-lived naked mole-rat, Sci. Rep. 7 (2017) 1–9, https://doi.org/10.1038/s41598-017-10287-0.
[14] M. Dziegelewska, S. Holtze, C. Vole, U. Wachter, U. Menzel, M. Morhart, et al., Low sulfide levels and a high degree of cystathionine β-synthase (CBS) activation by S-adenosylmethionine (SAM) in the long-lived naked mole-rat, Redox Biol. 8 (2016) 192–198, https://doi.org/10.1016/j.redox.2016.01.008.
[15] S. Holtze, S. Braude, A. Lemma, R. Koch, M. Morhart, K. Szafranski, et al., The microenvironment of naked mole-rat burrows in East Africa, Afr. J. Ecol. 56 (2017) 279–289, https://doi.org/10.1111/aje.12448.
[16] F.M. Clarke, C. Faulkes, Dominance and queen succession in captive colonies of the eusocial naked mole–rat, Heterocephalus glaber, Proc. R. Soc. Med. 264 (1997) 993–1000, https://doi.org/10.1098/rspb.1997.0137.
[17] M.A. Delaney, L. Nagy, M.J. Kinsel, P.M. Treuting, Spontaneous histologic lesions of the adult naked mole rat (Heterocephalus glaber), Vet. Pathol. 50 (2013) 607–621, https://doi.org/10.1177/0300985812471543.
[18] T.J. Park, J. Reznick, B.L. Peterson, G. Blass, D. Omerbasic, N.C. Bennett, et al., Fructose-driven glycolysis supports anoxia resistance in the naked mole-rat, Science 356 (2017) 305–308, https://doi.org/10.1126/science.aab3896.
[19] R. Buffenstein, J. Jarvis, L.A. Opperman, M. Cavaleros, F.P. Ross, J.M. Pettifor, Subterranean mole-rats naturally have an impoverished calciol status, yet synthesize calciol metabolites and calbindins, Eur. J. Endocrinol. 130 (1994) 402–409, https://doi.org/10.1530/eje.0.1300402.
[20] R. Buffenstein, I.N. Sergeev, J.M. Pettifor, Vitamin D hydroxylases and their regulation in a naturally vitamin D-deficient subterranean mammal, the naked mole rat (Heterocephalus glaber), J. Endocrinol. 138 (1993) 59–64, https://doi.org/10.1677/joe.0.1380059.
[21] S. Mori, D.B. Burr, Increased intracortical remodeling following fatigue damage, Bone 14 (1993) 103–109.
[22] V. Bentolila, T.M. Boyce, D.P. Fyhrie, R. Drumb, T.M. Skerry, M.B. Schaffler, Intracortical remodeling in adult rat long bones after fatigue loading, Bone 23 (1998) 275–281.
[23] F.L. Bach-Gansmo, S.C. Irvine, A. Brüel, J.S. Thomsen, H. Birkedal, Calcified cartilage islands in rat cortical bone, Calcif. Tissue Int. 92 (2013) 330–338, https://doi.org/10.1007/s00223-012-9682-6.
[24] V. Ip, Z. Toth, J. Chibnall, S. McBride-Gagyi, Remnant woven bone and calcified cartilage in mouse bone: differences between ages/sex and effects on bone strength, PLoS One 11 (2016) e0166476, , https://doi.org/10.1371/journal.pone.0166476.
[25] A. Shipov, P. Zaslansky, H. Riesemeier, G. Segev, A. Atkins, R. Shahar, Unremodeled endochondral bone is a major architectural component of the cortical bone of the rat (Rattus norvegicus), J. Struct. Biol. 183 (2013) 132–140, https://doi.org/10.1016/j.jsb.2013.04.010.
[26] M. Pinto, K.J. Jepsen, C.J. Terranova, R. Buffenstein, Lack of sexual dimorphism in femora of the eusocial and hypogonadic naked mole-rat: a novel animal model for the study of delayed puberty on the skeletal system, Bone 46 (2010) 112–120, https://doi.org/10.1016/j.bone.2009.08.060.
[27] G.P. Evans, J.C. Behiri, J.D. Currey, W. Bonfield, Microhardness and Young modulus in cortical bone exhibiting a wide-range of mineral volume fractions, and in a bone analog, J. Mater. Sci. Mater. Med. 1 (1990) 38–43, https://doi.org/10.1007/BF00705352.
[28] D.J. Daegling, J.L. Hotzman, W.S. McGraw, A.J. Rapoff, Material property variation of mandibular symphyseal bone in colobine monkeys, J. Morphol. 270 (2009) 194–204, https://doi.org/10.1002/jmor.10679.
[29] G. Robertson, C. Xie, D. Chen, H. Awad, E.M. Schwarz, R.J. O'Keefe, et al., Alteration of femoral bone morphology and density in COX-2 −/− mice, Bone 39 (2006) 767–772, https://doi.org/10.1016/j.bone.2006.04.006.
[30] J.M. Wallace, R.M. Rajachar, M.R. Allen, S.A. Bloomfield, P.G. Robey, M.F. Young, et al., Exercise-induced changes in the cortical bone of growing mice are bone- and gender-specific, Bone 40 (2007) 1120–1127, https://doi.org/10.1016/j.bone.2006.12.002.
[31] L.M. Miller, W. Little, A. Schirmer, F. Sheik, B. Busa, S. Judex, Accretion of bone quantity and quality in the developing mouse skeleton, Jbmr 22 (2007) 1037–1045, https://doi.org/10.1359/jbmr.070402.
[32] M.N. Cosman, H.M. Britz, C. Rolian, Selection for longer limbs in mice increases bone stiffness and brittleness, but does not alter bending strength, J. Exp. Biol. 222 (2019), https://doi.org/10.1242/jeb.203125.
[33] N. Rodriguez-Florez, E. Garcia-Tunon, Q. Mukadam, E. Saiz, K.J. Oldknow, C. Farquharson, et al., An investigation of the mineral in ductile and brittle cortical mouse bone, Jbmr 30 (2015) 786–795, https://doi.org/10.1002/jbmr.2414.
[34] J. Aerssens, S. Boonen, G. Lowet, J. Dequeker, Interspecies differences in bone composition, density, and quality: potential implications for in vivo bone research, Endocrinology. 139 (n.d.) 663–670.
[35] Y. Jiao, H. Chiu, Z. Fan, F. Jiao, E.C. Eckstein, W.G. Beamer, et al., Quantitative trait loci that determine mouse tibial nanoindentation properties in an F2 population derived from C57BL/6J x C3H/HeJ, Calcif. Tissue Int. 80 (2007) 383–390, https://doi.org/10.1007/s00223-007-9030-4.
[36] S. Viguet-Carrin, M. Hoppler, F. Membrez Scalfo, J. Vuichoud, M. Vigo, E.A. Offord, et al., Peak bone strength is influenced by calcium intake in growing rats, Bone 68 (2014) 85–91, https://doi.org/10.1016/j.bone.2014.07.029.
[37] G.-Z. Jiang, H. Matsumoto, M. Hori, A. Gunji, K. Hakozaki, Y. Akimoto, et al., Correlation among geometric, densitometric, and mechanical properties in mandible and femur of osteoporotic rats, J. Bone Miner. Metab. 26 (2008) 130–137, https://doi.org/10.1007/s00774-007-0811-7.
[38] V. Canè, G. Marotti, G. Volpi, D. Zaffe, S. Palazzini, F. Remaggi, et al., Size and density of osteocyte lacunae in different regions of long bones, Calcif. Tissue Int. 34 (2006) 558–563.
[39] R. Dai, Y. Ma, Z. Sheng, Y. Jin, Y. Zhang, L. Fang, et al., Effects of genistein on vertebral trabecular bone microstructure, bone mineral density, microcracks, osteocyte density, and bone strength in ovariectomized rats, J. Bone Miner. Metab. 26 (2008) 342–349, https://doi.org/10.1007/s00774-007-0830-4.
[40] C.J. Hernandez, R.J. Majeska, M.B. Schaffler, Osteocyte density in woven bone, Bone 35 (2004) 1095–1099, https://doi.org/10.1016/j.bone.2004.07.002.
[41] E.M. Aarden, E.H. Burger, P.J. Nijweide, Function of osteocytes in bone, J. Cell. Biochem. 55 (1994) 287–299, https://doi.org/10.1002/jcb.240550304.
[42] S. Mishra, M.L. Knothe Tate, Effect of lacunocanalicular architecture on hydraulic conductance in bone tissue: implications for bone health and evolution, Anat Rec A Discov Mol Cell Evol Biol 273 (2003) 752–762, https://doi.org/10.1002/ar.a.10079.
[43] L.E. Lanyon, Osteocytes, strain detection, bone modeling and remodeling, Calcif. Tissue Int. 53 (Suppl. 1) (1993) S102–6– discussion S106–7.
[44] J.D. Currey, M.N. Dean, R. Shahar, Revisiting the links between bone remodelling and osteocytes: insights from across phyla, Biol. Rev. Camb. Philos. Soc. 92 (2017) 1702–1719, https://doi.org/10.1111/brv.12302.
[45] P. Christiansen, Mass allometry of the appendicular skeleton in terrestrial mammals, J. Morphol. 251 (2001) 195–209, https://doi.org/10.1002/jmor.1083.
[46] A.A. Biewener, Allometry of quadrupedal locomotion - the scaling of duty factor, bone curvature and limb orientation to body size, J. Exp. Biol. 105 (1983) 147–171.
[47] A.A. Biewener, Bone strength in small mammals and bipedal birds - do safety factors change with body size, J. Exp. Biol. 98 (1982) 289–301.
[48] A.A. Biewener, Mammalian terrestrial locomotion and size, Bioscience 39 (1989) 776–783, https://doi.org/10.2307/1311183.
[49] R.M. Alexander, Factors of safety in the structure of animals, Sci. Prog. 67 (1981) 109–130.
[50] C.G. Faulkes, D.H. Abbott, J.U. Jarvis, F.E. Sherriff, LH responses of female naked mole-rats, Heterocephalus glaber, to single and multiple doses of exogenous GnRH, J. Reprod. Fertil. 89 (1990) 317–323.
[51] J. Jarvis, M. O'Riain, E. McDaid, Growth and Factors Affecting Body Size in Naked Mole-rats, (1991).
[52] C.M. Dengler-Crish, K.C. Catania, Phenotypic plasticity in female naked mole-rats after removal from reproductive suppression, J. Exp. Biol. 210 (2007) 4351–4358, https://doi.org/10.1242/jeb.009399.